



1 **Zeppelin-led study on the onset of new particle formation in the planetary boundary layer**

2

3 Janne Lampilahti¹, Hanna E. Manninen², Tuomo Nieminen¹, Sander Mirme³, Mikael Ehn¹, Iida
4 Pullinen⁴, Katri Leino¹, Siegfried Schobesberger^{1,4}, Juha Kangasluoma¹, Jenni Kontkanen¹, Emma
5 Järvinen⁵, Riikka Väänänen¹, Taina Yli-Juuti⁴, Radovan Krejci⁶, Katrianne Lehtipalo^{1,7}, Janne
6 Levula¹, Aadu Mirme³, Stefano Decesari⁸, Ralf Tillmann⁹, Douglas R. Worsnop^{1,4,10}, Franz Rohrer⁹,
7 Astrid Kiendler-Scharr⁹, Tuukka Petäjä^{1,11}, Veli-Matti Kerminen¹, Thomas F. Mentel⁹, and Markku
8 Kulmala^{1,11,12}

9

10 ¹Institute for Atmospheric and Earth System Research / Physics, Faculty of Science, University of
11 Helsinki, Helsinki, Finland.

12 ²CERN, CH-1211 Geneva, Switzerland.

13 ³Institute of Physics, University of Tartu, Tartu, Estonia.

14 ⁴Department of Applied Physics, University of Eastern Finland, Kuopio, Finland.

15 ⁵National Center for Atmospheric Research, Boulder, CO, USA.

16 ⁶Department of Environmental Science & Bolin Centre for Climate research, Stockholm University,
17 Stockholm, Sweden.

18 ⁷Finnish Meteorological Institute, Helsinki, Finland.

19 ⁸Istituto di Scienze dell'Atmosfera e del Clima, CNR, Bologna, Italy.

20 ⁹Institute for Energy and Climate Research, IEK-8, Forschungszentrum Jülich GmbH, Jülich,
21 Germany.

22 ¹⁰Aerodyne Research Inc, Billerica, MA, USA.

23 ¹¹Joint International Research Laboratory of Atmospheric and Earth System Sciences, Nanjing
24 University, Nanjing, China.

25 ¹²Aerosol and Haze Laboratory, Beijing Advanced Innovation Center for Soft Matter Science and
26 Engineering, Beijing University of Chemical Technology, Beijing, China.

27

28 Correspondence to: Janne Lampilahti (janne.lampilahti@helsinki.fi)

29

30 **Abstract**

31 We compared observations of aerosol particle formation and growth in different parts of the
32 planetary boundary layer at two different environments that have frequent new particle formation
33 (NPF) events. In summer 2012 we had a campaign in Po Valley, Italy (urban background) and in
34 spring 2013 a similar campaign took place in Hyytiälä, Finland (rural background). Our study



35 consists of airborne and ground-based measurements of ion and particle size distribution from ~1
36 nm. The airborne measurements were performed using a Zeppelin inside the boundary layer up to
37 1000 m altitude. Our observations show the onset of regional NPF and the subsequent growth of the
38 aerosol particles happening uniformly inside the mixed layer (ML) in both locations. However, in
39 Hyttiälä we noticed local enhancement in the intensity of NPF caused by mesoscale BL dynamics.
40 Additionally, our observations indicate that in Hyttiälä NPF was probably also taking place above
41 the ML. In Po Valley we observed NPF that was limited to a specific air mass.

42

43 **1 Introduction**

44 The boundary layer (BL) is the lowest layer of the earth's atmosphere (Stull, 1988). The BL is an
45 interface controlling the exchange of mass and energy between atmosphere and surface. Ground
46 based measurements are often used as representative observations for the whole BL. However they
47 cannot cover vertical internal variability of BL and this can be addressed only by airborne
48 observations.

49

50 Figure 1 show the typical BL evolution over land during the time span on one day. Shortly after
51 sunrise convective mixing creates a mixed layer (ML) that rapidly grows during the morning by
52 entraining air from above and can reach an altitude of ~1-2 km above the surface. The ML is capped
53 by a stable layer at the top. Above the BL is the free troposphere (FT), which is decoupled from the
54 surface. Here we define BL to mean all the layers below the FT. Around sunset convective mixing
55 and turbulence diminishes and the ML becomes what is known as the residual layer (RL). During
56 the night a stable boundary layer develops due to interaction with the ground surface. This layer has
57 only weak intermittent turbulence and it smoothly blends into the RL.

58

59 We studied where new particle formation (NPF) occurs in the BL and how it relates to BL
60 evolution, comparing two different environments. NPF refers to the formation of nanometer sized
61 clusters from low-volatility vapors present in the atmosphere, and their subsequent growth to larger
62 aerosol particles (Kulmala et al., 2013). Understanding NPF better is of major interest, since it is a
63 dominant source of cloud condensation nuclei in the atmosphere and therefore can have important
64 indirect effects on climate (Dunne et al., 2016; Gordon et al., 2017; Pierce and Adams, 2009; Yu and
65 Luo, 2009).

66

67 Nilsson et al. (2001) studied NPF in a boreal forest environment and observed that in addition to
68 increased solar radiation the onset of turbulence appears to be a necessary trigger for NPF. Several



69 explanations for this connection were proposed: NPF might be starting in the RL or at the top of the
70 shallow ML, from where the aerosol particles are mixed to the surface as the ML starts to grow.
71 NPF starts in the ML due to dilution of pre-existing aerosol and drop in vapor sink. Convective
72 mixing brings different precursor gases, one present in the RL and the other in the ML, into contact
73 with each other initiating NPF inside the ML.

74

75 Airborne measurements of nanoparticles from different environments show that NPF occurs in
76 many parts of the BL. Multiple observations from Central Europe suggest that aerosol particles are
77 formed on top of a shallow ML (Platis et al., 2015; Siebert et al., 2004; Chen et al., 2018) or inside
78 the RL (Stratmann et al., 2003; Wehner et al., 2010). Other results come from a boreal forest
79 environment in southern Finland. Lampilahti et al. (2020a) showed evidence that NPF may occur in
80 the interface between the RL and the FT. O'Dowd et al. (2009) observed the first signs of NPF in
81 the surface ML and Leino et al. (2019) showed that sub-3 nm particles have higher concentration
82 close to surface. Laakso et al. (2007) performed hot-air balloon measurements and concluded that
83 NPF either took place throughout the ML or in the lower part of the ML. Measurements by
84 Schobesberger et al. (2013) suggested that NPF was more intense in the top parts of a developed
85 ML. More measurements are needed in order to understand these mixed results.

86

87 Here we present NPF measurements on board a Zeppelin airship carried out during the EU
88 supported PEGASOS (Pan-European Gas-AeroSOls Climate Interaction Study) project. The main
89 goal of the project was to quantify the magnitude of regional to global feedbacks between
90 atmospheric chemistry and physics, and thus quantify their impact on the changing climate. The
91 Zeppelin flights were used to observe radicals, trace gases, and aerosol particles inside the lower
92 troposphere over Europe in several locations during 2012-2013.

93

94 By using a Zeppelin NT (Neue Technologie) airship we were able to sample from a stable, agile
95 platform, up to 1000 meters above sea level (asl). The high payload capacity of the Zeppelin
96 enabled us to carry state-of-the-art instrumentation, specifically designed to collect information on
97 the feedback processes between the chemical compounds and the smallest aerosol particles to better
98 estimate their role in climate and air quality.

99

100 The NPF focused campaigns presented here were performed in Po Valley, Italy, and Hyytiälä,
101 Finland. At both locations NPF events happen frequently. Po Valley represents urban background
102 conditions where anthropogenic emissions are an important source of gaseous precursors for NPF



103 (e.g. Kontkanen et al., 2016). Hyytiälä represents rural background conditions where organic vapors
104 from the surrounding forests play a major role in NPF (e.g. Dada et al., 2017).

105

106 Here we combine comprehensive ground-based and airborne measurements to compare two NPF
107 cases from Po Valley to one case from Hyytiälä. The Zeppelin allowed us to repeatedly profile the
108 lowest 1 km of the atmosphere providing a full picture of what is happening in the BL during the
109 onset of NPF. We will show in which part or parts of the BL the onset of NPF and the subsequent
110 particle growth occurred at the two measurement sites as well as determine formation and growth
111 rates for the aerosol particles.

112

113 **2 Methods**

114 San Pietro Capofiume in Po Valley, Italy and Hyytiälä in Southern Finland are interesting
115 environments to compare from nucleation and particle growth point of view because NPF is
116 frequently observed in both environments. The vertical measurement profiles analyzed in this study
117 were performed in a close proximity to the ground-based measurement sites.

118

119 **2.1 San Pietro Capofiume, Italy**

120 San Pietro Capofiume (SPC, 44°39'N 11°37'E, 11 m asl) is located in the eastern part of Po Valley,
121 Italy, between the cities of Bologna and Ferrara. Po Valley is considered a pollution hot spot,
122 although, the station itself is surrounded by vast agricultural fields away from point sources. Thus
123 the aerosol concentration and composition at SPC reflect the Po Valley regional background. NPF is
124 frequently observed in SPC (36% of days) with maxima in May and July (Hamed et al., 2007;
125 Laaksonen et al., 2005).

126

127 The instruments measuring the aerosol particle number-size distribution were a scanning mobility
128 particle sizer (SMPS, 10-700 nm, 5 min time resolution; Wiedensohler et al., 2012) and a neutral
129 cluster and air ion spectrometer (NAIS, particles: ~2-40 nm, ions: 0.8-40 nm, 4 min time resolution;
130 Mirme and Mirme, 2013). We used the NAIS's positive polarity for the particle number size
131 distribution data. The ML height was determined from ceilometer (Lufft CHM 15k) measurements.
132 Basic meteorology and SO₂ gas concentration data (Thermo 43iTLE monitor) were also available at
133 surface level (2-3 m above ground level).

134

135 **2.2 Hyytiälä, Finland**



136 In Finland the ground-based measurements were performed at the SMEAR II (Station for
137 Measuring Forest Ecosystem-Atmosphere Relations II) station located in Hyytiälä, Finland (HTL,
138 61°51'N 24°17'E, 181 m asl; Hari and Kulmala, 2005). The station is equipped with extensive
139 facilities to measure the forest ecosystem and the atmosphere. The measurement site is surrounded
140 by coniferous boreal forest.

141

142 The forest emits biogenic volatile organic compounds (Hakola et al., 2003), which can be oxidized
143 in the atmosphere to form low-volatile vapors that contribute to aerosol particle formation and
144 growth (Ehn et al., 2014; Mohr et al., 2019). NPF is frequently observed in HTL (23% of all days),
145 especially in spring and autumn (Dal Maso et al., 2005; Nieminen et al., 2014).

146 Aerosol particle and ion number-size distributions were measured by the station's differential
147 mobility particle sizer (DMPS, 3-1000 nm, 10 min time resolution; Aalto et al., 2001) and the NAIS
148 (Manninen et al., 2009). Sub-3 nm particle number-size distribution was measured by a particle size
149 magnifier running in scanning mode (PSM, 1.2-2.5 nm, 10 min time resolution; Vanhanen et al.,
150 2011). Also a PSM measured at SPC but we were not able to reliably calculate formation rates from
151 the data. Basic meteorological variables, radiation, and SO₂ were measured from the station's mast
152 at 16.8 meters above ground. In addition, a supporting NPF forecast tool was developed to aid the
153 planning of research flights (Nieminen et al., 2015).

154

155 **2.3 Zeppelin NT airship**

156 A Zeppelin NT airship was used for monitoring the atmosphere below 1 km. The aerosol particles
157 and trace gases were sampled with instrumentation installed inside the Zeppelin's cabin. The
158 Zeppelin operated with three different instrument layouts. A specific layout was chosen according to
159 the flight plan and scientific aim of the flight.

160

161 Here we analyzed data from measurement flights that carried the so-called nucleation layout.
162 Instruments specific to this layout were the atmospheric pressure interface time-of-flight mass
163 spectrometer (APi-TOF; Junninen et al., 2010), used for measuring the elemental composition of
164 naturally charged ions and the NAIS for particle and ion number size distributions. We also used the
165 aerosol number-size distribution data from the SMPS (10-400 nm, 4 min time resolution) and PSM
166 running in scanning mode, which were on board during all the measurement flights. The size range
167 and time resolution of the onboard NAIS and PSM were same as for the instruments in HTL (see
168 Section 2.1).

169



170 During a measurement flight the Zeppelin did multiple vertical profiles over a small area ($\sim 10 \text{ km}^2$).
171 The profiling spot was picked typically down-wind from the measurement site in order not to
172 compromise the ground-based measurements with any emissions. The vertical extent of the profiles
173 was $\sim 100\text{-}1000 \text{ m}$ above the ground. The airspeed during measurement was $\sim 20 \text{ m/s}$ and the
174 vertical speed during ascend and descend was $\sim 0.5 \text{ m/s}$ and $\sim 3 \text{ m/s}$ respectively.

175

176 **2.4. Cessna 172 airplane**

177 During the PEGASOS northern mission in spring 2013, a Cessna 172 airplane carrying scientific
178 instrumentation was deployed to measure aerosol particles, trace gases and meteorological variables
179 in the lower troposphere alongside the Zeppelin. The measurement setup and instrumentation on
180 board have been described in previous studies (Schobesberger et al., 2013; Lampilahti et al., 2020c;
181 Leino et al., 2019; Väänänen et al., 2016).

182

183 Basic meteorological variables (temperature, pressure, relative humidity) were measured on board.
184 Particle number-size distribution was measured using a SMPS (10-400 nm size range, 2 min time
185 resolution) and the number concentration of $>3 \text{ nm}$ particles was measured using an ultrafine
186 condensation particle counter (UF-CPC, TSI model 3776) at 1 s time resolution. The altitude range
187 of the airplane was $\sim 100\text{-}3000 \text{ m}$ above ground and the measurement airspeed was 36 m/s .

188

189 **2.5 Flight profiles and atmospheric conditions**

190 Our measurements focused on the time of BL development from sunrise until noon (Figure 1). This
191 is the time when the onset of NPF is typically observed at the ground level. The vertical profile
192 measurements represent the particle and gas concentrations in the lower parts of the atmosphere: the
193 mixed layer, the residual layer, the nocturnal boundary layer. At the same time, the ground-based
194 measurements recorded conditions in the surface layer. Here we consider the BL to include all the
195 atmospheric layers below the free troposphere.

196

197 The basic conditions for the Zeppelin flights in both Italy and Finland were clear sky and low wind
198 speed. Under these conditions, the sun heats the surface during the morning, which drives intense
199 vertical mixing.

200

201 **2.6 Data analysis**

202 The onset of NPF occurs when low-volatility vapors in the atmosphere form nanometer sized
203 clusters that continue to grow to larger aerosol particles (Kulmala et al., 2013).



204

205 We determined the onset of a NPF event visually from the initial increase in the number
206 concentration of intermediate (2-4 nm) air ions at the beginning of the NPF event. An increase in
207 the intermediate ion concentration has been identified as a good indicator for NPF (Leino et al.,
208 2016). This is because an increase in the number concentration of intermediate ions is usually due
209 to NPF and otherwise the number concentration is extremely low (below 5 cm^{-3}).

210

211 Particle growth rates (GR), formation rates and coagulation sinks were calculated in different size
212 ranges according to the methods described by Kulmala et al. (2012). For particles and ions in the 1-
213 2 nm and 2-3 nm size range the GR was determined from the ion number-size distribution measured
214 by the NAIS. During NPF the number concentration in each size channel increased sequentially as
215 the freshly formed particles grew larger. We determined the time when the number concentration
216 began to rise in each size bin by fitting a sigmoid function to the rising concentration edge and
217 finding the point where the sigmoid reached 75% of its maximum value (appearance time method;
218 Lehtipalo et al., 2014). The corresponding diameter in each size bin was the bin's geometric mean
219 diameter. Before the fitting procedure the number concentrations were averaged using a 15 min
220 median and after that divided by the maximum concentration value in each size channel.

221

222 For larger particles and ions (3-7 nm and 7-20 nm) the GR was determined by fitting a log-normal
223 distribution over the growing nucleation mode at each time step and assigning the fitted curve's
224 peak value as the corresponding mode diameter. In each size range a value for the GR was obtained
225 as the slope of a linear least squares fit to the time-diameter value pairs.

226

227 The formation rate of 1.5 nm particles and ions was determined from the PSM data and the NAIS
228 ion data respectively (Kulmala et al., 2012). The formation rate of 3 nm particles and ions was
229 determined from the NAIS data. Coagulation sinks were calculated from the SMPS or DMPS data.
230 Condensation sink for sulfuric acid was calculated from the Zeppelin's on board SMPS.

231

232 Sulfuric acid (SA) is a key compound in atmospheric nucleation (Sipilä et al., 2010). As we did not
233 have direct measurements of SA concentration, we used $[\text{HSO}_4^-]$ from the APi-TOF measurements
234 as a qualitative indicator of $[\text{H}_2\text{SO}_4]$ and named it pseudo-SA. To determine this pseudo-SA, we
235 summed up all ions containing HSO_4^- , e.g. the ion itself but also larger clusters, like
236 $(\text{H}_2\text{SO}_4)_n \cdot \text{HSO}_4^-$. We assumed steady state conditions and that the concentration of SA-containing
237 ions is much lower than the total ion concentration. Under these conditions $[\text{HSO}_4^-]$ (including all



238 clusters where this ion was present) can be considered close to a linear function of $[H_2SO_4]$ (Eisele
239 and Tanner, 1991). At the highest SA loadings, ions with HSO_4^- can be a dominant fraction of the
240 total ions (Ehn et al., 2010), in which case the linearity no longer holds. In addition, this assumes a
241 constant concentration of ions, although for example the sinks for ions can vary, e.g. by an
242 increased particle concentration. As such, the pseudo-SA parameter should indeed only be
243 considered a qualitative indicator for SA.

244

245 In SPC the ML height was derived from the ceilometer measurements. However, in HTL weak
246 scattering signal prevented reliable determination of ML height using the on-site lidar. For this
247 reason in HTL the ML height was determined from vertical profiles of meteorological variables and
248 aerosol particle concentrations on board the Zeppelin and the Cessna 172 airplane. In these profiles
249 the top of the ML was revealed by the maximum positive gradient in potential temperature and
250 minimum negative gradient in humidity and total particle number concentration (Stull, 1988).

251

252 The origin of the air masses was investigated using back trajectory analysis. The trajectories were
253 calculated with the HYSPLIT (Hybrid Single Particle Lagrangian Integrated Trajectory; Stein et al.,
254 2015) model using the GDAS (Global Data Assimilation System) archived data sets.

255

256

257 **3 Results and discussion**

258

259 **3.1 Case study description**

260 During the campaigns there were a limited number of flights with the nucleation instrument
261 payload. Here we present a side by side comparison of two case studies, one from SPC (June 28,
262 2012) and the other from HTL (May 8, 2013). In addition the horizontal extent of NPF in SPC was
263 investigated by studying the research flight from June 30, 2012.

264

265 June 28, 2012 was a hot and sunny day in Po Valley. 24-h back trajectories arriving to SPC during
266 the morning revealed that the incoming air masses circulated from Central Europe and over the
267 Adriatic Sea before arriving to SPC from the southwest (Figure 2a). Figure 3 shows the time series
268 for some environmental parameters on the NPF event days from SPC and HTL. In SPC temperature
269 and RH showed a large diurnal variation; the temperature increased from 16 °C to 32 °C during the
270 morning while the RH decreased from 87% to 39%. The mean wind speed at 10 m height was 2.0 m



271 s^{-1} . These meteorological conditions and air mass histories are common during NPF event days in
272 Po Valley (Hamed et al., 2007; Sogacheva et al., 2007).

273

274 May 8, 2013 in HTL was a sunny and warm day with clear skies marked by broad diurnal variation
275 in temperature and RH. During the morning the temperature increased from 5 °C to 17 °C and the
276 RH decreased from 82% to 25%. The mean wind speed at 33.6 m height was 3.5 m s^{-1} . The air
277 masses originated from the North Atlantic Ocean arriving to HTL from the northwest via
278 Scandinavia and the Gulf of Bothnia (Figure 2b). Most NPF event days in HTL are clear sky days
279 with the arriving air masses spending most of their time in the northwest sector (Dada et al., 2017;
280 Nilsson et al., 2001; Sogacheva et al., 2008).

281

282 In SPC the solar radiation began to increase after 04:00 and the ML started to increase in height
283 around 06:00, at the same time the SO_2 concentration and $N_{>10}$ (number concentration of particles
284 larger than 10 nm) began to increase. This is likely explained by the entrainment of pollutants from
285 the RL and the onset of NPF. CS is higher during the night and decreases slightly during the day,
286 which is likely due to dilution related to ML growth.

287

288 At HTL after sunrise the SO_2 concentration and $N_{>10}$ decreased probably due to the dilution caused
289 by the growing ML coupled with the lack of pollution sources. While SO_2 concentration remained
290 low the whole day, $N_{>10}$ and CS began to increase later during the day because of the NPF event.
291 The average SO_2 , $N_{>10}$ and CS in SPC were 0.57 ppb, 8102 cm^{-3} and 0.0128 s^{-1} respectively. While
292 in HTL the corresponding values were 0.02 ppb, 3293 cm^{-3} and 0.0007 s^{-1} .

293

294 **3.2 Onset of NPF**

295 Figures 4a and 4b show the altitude of the Zeppelin as a function of time colored by the number
296 concentration of intermediate ions measured by the NAIS at SPC and HTL. The plots also show the
297 number concentration of intermediate ions measured on the ground as well as the ML height.

298

299 In SPC, the intermediate ion concentration began to increase on the ground at 5:48, which coincides
300 with the beginning of convective mixing and the breakup of the nocturnal surface layer. Similarly,
301 Kontkanen et al. (2016) observed that in Po Valley the onset of NPF coincided with the beginning
302 of boundary layer growth. Around this time the Zeppelin was profiling the layers above the ML.
303 “Pockets” of elevated intermediate ion concentration were present inside the RL (for example
304 around 700 m at 5:15). These pockets were not linked to the NPF event inside the ML. When the



305 Zeppelin later entered the ML at around 6:45, NPF was already taking place throughout the
306 developing ML and seemed to be confined to it.

307

308 In HTL, the number concentration of intermediate ions began to increase at around 6:47 on the
309 ground level. The ML at this point had grown to around 600 m above ground, which allowed us to
310 better resolve the onset of NPF vertically. In HTL no increase in intermediate ion concentration,
311 indicating no NPF, was observed above the ML on board the Zeppelin. Before 6:40 there was no
312 sign of NPF inside the growing ML. Between 6:40 and 7:00 the Zeppelin briefly measured in the
313 RL and re-entered the ML at 7:00. At this point the intermediate ion concentration was already
314 increasing on board similar to the ground level, indicating the onset of NPF.

315

316 Figure 5 shows the intermediate ion number concentration as a function of time from the Zeppelin
317 and the SMEAR II station. At the beginning of the NPF event, between 07:00-07:15, the Zeppelin
318 ascended from 300 m to 800 m. During the ascend the intermediate ion concentrations increased at
319 a similar rate and stayed at similar values on board the Zeppelin and at the ground level. The lack of
320 vertical gradient in the number concentration suggests that the aerosol particles were forming
321 homogeneously throughout the ML. However, intense turbulent mixing and strong updrafts moving
322 up at roughly the same rate as the Zeppelin might have also resulted in a homogeneous number
323 concentration, even if the aerosol particles were formed close to the surface.

324

325 Figures 4c and 4d show the Zeppelin's measurement profiles colored with the pseudo SA. In SPC,
326 the highest amount of pseudo SA appears to be in the residual layer above the growing morning ML
327 (also observed on June 27, 2012) after sunrise. This is in line with the observation that the SO₂
328 concentration increases at the surface when the ML starts to grow (Figure 3b), indicating that the
329 SO₂ was entrained from the RL. The entrainment of SO₂ from the residual layer is also supported by
330 previous observations (Kontkanen et al., 2016). The increased pseudo SA in the residual layer was
331 not associated with NPF in the residual layer.

332

333 In SPC the night time SO₂ concentration at the surface is low likely due to deposition (Kontkanen et
334 al., 2016). However ammonia concentration can be high (>30 µg m⁻³) at the surface due to
335 agricultural activities and the concentration has been observed to peak during the night and early
336 morning (Sullivan et al., 2016).

337



338 Since in SPC the onset of NPF coincides with the beginning of ML growth, it is possible that the
339 entrainment of SA from the residual layer into the growing ML where ammonia, and likely also
340 amines from agricultural activities, are present can lead to stabilization of the SA clusters by the
341 ammonia and amines and subsequent NPF (e.g. Almeida et al., 2013; Kirkby et al., 2011).

342

343 In SPC the pseudo-SA layer closely corresponded to a layer of reduced condensation sink (CS). In
344 low CS regions more SA is in the gas phase and therefore detected by the APi-TOF (Figures 4e and
345 4f), which probably explains why the layer is there. In addition, the CS is also a sink for ions, which
346 means that the pseudo-SA is likely decreased even more than SA, assuming that the loss rate is
347 higher for ions than for SA molecules. By contrast, in HTL the amount of pseudo-SA is higher
348 inside the ML than above it. The pseudo-SA concentration increases on board throughout the
349 morning and peaks at roughly 9:00 and decreases afterwards.

350

351 In SPC pockets of intermediate ions and a layer of pseudo SA were observed in the RL, whereas at
352 HTL intermediate ion concentrations and pseudo SA remained low in the RL. This is likely related
353 to the relatively larger anthropogenic emissions in the Po Valley region compared to HTL. In
354 previous studies NPF has been observed inside the RL in Central Europe (Wehner et al., 2010) and
355 primary nanoparticles may be released into the RL from upwind pollution sources (Junkermann and
356 Hacker, 2018).

357

358 **3.2 Particle formation and growth rates**

359 Figure 6 shows the number size distributions measured by the NAIS on board the Zeppelin and on
360 the ground from SPC and HTL. The black dots are the mean mode diameters obtained by fitting a
361 log-normal distribution over the growing particle mode.

362

363 In SPC, the number size distributions measured on board and on the ground with the NAIS (Figures
364 6a and 6c) were similar when the Zeppelin was measuring inside the ML. When the Zeppelin
365 measured above the ML the number concentration decreased and the growing mode of freshly
366 formed particles was not observed. The pockets of intermediate ions in the RL did not grow to
367 larger sizes. This can be seen as sudden disappearances of the particles, for example at around 6:40,
368 7:15 and 8:00. The observations suggests that the NPF event was limited to the ML where it was
369 taking place homogeneously.

370



371 We calculated the formation and growth rates in SPC and HTL for particles and ions on board the
372 Zeppelin and on the ground. The results are summarized in Table 1. In SPC the onset of NPF
373 happened when the ML was still very shallow and the Zeppelin was not measuring significant
374 amount of time at this low altitude (this was a problem on other NPF event days from SPC as well),
375 consequently the beginning of the NPF event was not fully observed on board. Because of this we
376 were unable to reliably calculate the formation rates and the growth rate between 1-2 nm from the
377 Zeppelin data.

378

379 Kontkanen et al. (2016) obtained formation rates of $23.5 \text{ cm}^{-3} \text{ s}^{-1}$, $9.5 \text{ cm}^{-3} \text{ s}^{-1}$, $0.1 \text{ cm}^{-3} \text{ s}^{-1}$ and 0.08
380 $\text{cm}^{-3} \text{ s}^{-1}$ for 1.5 nm particles, 2 nm particles, 2 nm positive ions and 2 nm negative ions respectively
381 for the June 28, 2012 NPF event at the ground level. These values are in line with our values for the
382 same day reported in Table 1 ($J_3 = 6.8 \text{ cm}^{-3}$, $J_3^- = 0.04 \text{ cm}^{-3}$, $J_3^+ = 0.03 \text{ cm}^{-3}$). The higher formation
383 rates in SPC compared to HTL are characteristic of polluted environments (Kerminen et al., 2018).
384 The calculated GRs for the larger particle sizes as seen in Table 1 were similar on board the
385 Zeppelin (HTL: $\text{GR}_{7-20} = 2.4 \text{ nm/h}$, SPC: $\text{GR}_{7-20} = 3.0 \text{ nm/h}$) and on the ground (HTL: $\text{GR}_{7-20} = 2.1$
386 nm/h , SPC: $\text{GR}_{7-20} = 2.8 \text{ nm/h}$).

387

388 On May 8, 2013 in HTL almost the whole NPF event was captured by the Zeppelin measuring
389 inside the ML. However, in contrast to SPC the number size distributions measured on board the
390 Zeppelin (Figure 6b) and on the ground (Figure 6d) show differences, particularly in the growing
391 nucleation mode particles. At different times on board the Zeppelin when it was measuring inside
392 the ML the particle number concentration in the growing mode momentarily increased up to eight
393 fold compared to the background number concentration, suggesting an enhancement in the particle
394 formation rate. On board the Zeppelin this can be seen as concentrated "vertical stripes" in the
395 number size distribution between 08:00-10:00. On the other hand at the ground station an increase
396 of concentration of freshly formed particles was observed between 7:30-8:00. This inhomogeneity
397 is further discussed in Section 3.3.

398

399 In the ground-based NAIS data a pool of sub-6 nm particles was present during the NPF event
400 while on board the Zeppelin no such pool was observed. This can be seen most clearly between
401 10:00-11:30 when the median particle number concentration between 2-4 nm on the ground was
402 1400 cm^{-3} whereas on board the Zeppelin it was 570 cm^{-3} . Similarly Leino et al. (2019) observed
403 that the number concentration of sub-3 nm particles decreases as a function of altitude at HTL. This



404 may be linked to increased concentration of low-volatility vapors on the surface near the sources
405 compared to aloft.

406

407 Despite the differences in the ground-based and airborne number size distributions in HTL a
408 continuous, growing, nucleation mode was observed in the "background" both on the ground
409 (alongside the pool of sub-6 nm particles) and on board the Zeppelin during the NPF event. When
410 averaged over the total duration of the NPF event, the growth rates and formation rates on board the
411 Zeppelin and on the ground were similar on this day. This would indicate that the ground-based
412 measurements represent the NPF event in the whole ML quite well. However locally increased
413 number concentrations, indicating enhanced NPF, were observed inside the ML and if the
414 enhancement is not detected with the ground-based measurements we may underestimate the
415 intensity of NPF within the ML based on ground-based data alone.

416

417 **3.3 Vertical and horizontal distribution of the freshly formed particles**

418 Next we investigated how the freshly formed particles were distributed spatially in the BL. Figure 7
419 shows the particle number concentration between 3-10 nm measured by the NAIS and the ML
420 height from SPC as a function of time and altitude. The freshly formed particles were distributed
421 homogeneously throughout the growing ML but were not found in the RL. The 3-10 nm number
422 concentration inside the ML was $\sim 20\,000\text{ cm}^{-3}$ while in the residual layer it was only $\sim 200\text{ cm}^{-3}$. The
423 pockets of increased intermediate ion concentration, indicating NPF in the nocturnal boundary layer
424 and residual layer (Figure 4a), were not observed in the 3-10 nm size range suggesting that the
425 particles did not grow to the 3-10 nm size range in any significant numbers.

426

427 At HTL the Zeppelin was measuring in the lower half of the developed ML, however the Cessna
428 profiled the entire depth of the ML all the way up to the lower parts of the free troposphere. Figure
429 8 shows the vertical profile of 3-10 nm particle number concentration between 07:00-10:00 UTC
430 calculated by subtracting the total SMPS number concentration from the UF-CPC number
431 concentration on board the Cessna. Also the water vapor concentration and temperature are shown.
432 A temperature inversion, a large negative gradient in water vapor concentration and in the particle
433 number concentration indicated that the top of the ML was present between 1300-1400 m.

434

435 On average the number concentration inside the ML remained roughly constant ($N_{3-10} \sim 1000\text{ cm}^{-3}$)
436 as a function of altitude, however there was substantial variation ($\sim 200\text{-}3000\text{ cm}^{-3}$). The strongest
437 variation came from a narrow sector roughly at the center of the measurement area, which is



438 discussed below. The NPF did not extend to the RL where the number concentrations were reduced
439 to below 100 cm^{-3} .

440

441 However at 2000 m a layer of sub-10 nm particles was observed. The 3-10 nm number
442 concentration increased from less than 100 cm^{-3} to $\sim 400 \text{ cm}^{-3}$. Lampilahti et al. (2020a) showed
443 evidence that NPF frequently takes place in the interface between the residual layer and the free
444 troposphere, disconnected from the ML. Precursor gases may be transported to these altitudes and
445 the mixing over the interface layer could initiate nucleation.

446

447 Figure 9a shows the particle number concentration between 3-10 nm on board the Zeppelin and the
448 airplane as a function of longitude and latitude from HTL on May 8, 2013. The particle number
449 concentration was elevated right over HTL in a narrow sector perpendicular to the mean wind
450 direction. Vertically the sector extended throughout the depth of the ML. The number concentration
451 in the sector increased 2-8 fold compared to the surrounding background number concentration. The
452 mean wind speed in the ML was about 4 m/s and the particle sector was observed throughout the
453 whole measurement flight, for at least 2.5 hours. This suggests that the particle sector was probably
454 at least 35 km long along the mean wind direction.

455

456 The concentrated vertical stripes over the growing nucleation mode in Figure 6b were caused by the
457 Zeppelin periodically flying through the particle sector. The sector slowly moved perpendicular to
458 the mean wind towards northeast and when passing over HTL it was seen as the plume of particles
459 in Figure 6d between 07:30-08:00. The particles in the sector grew at approximately the same rate
460 with the background NPF event particles, which also suggests that the particles were formed
461 simultaneously inside the long and narrow sector. Lampilahti et al. (2020b) showed that these types
462 of NPF events, or local enhancements of regional NPF events, are common in HTL and that they
463 are linked to roll vortices, which are a specific mode of organized convection in the BL.

464

465 On June 28, 2012 in SPC the Zeppelin flew the measurement profiles over a small area and
466 therefore it was difficult to infer the horizontal extent of the NPF event. However, on June 30, 2012
467 the Zeppelin measured over a larger area in order to find the edges of the airmass where the NPF
468 event was taking place. The flight on June 30, 2012 lasted from 05:00 to 10:00 UTC. Figure 9b
469 shows that the NPF event was observed to occur in the sector of the Valley comprised between
470 Ozzano (just north of the Apennine foothills) and the city of Ferrara (just south of the Po river). The



471 area in between experienced westerly winds, from the inner Po Valley toward the Adriatic sea,
472 which is a common feature of the Po Valley wind breeze system in the early morning.
473
474 Farther north of the Po river, an easterly breeze was developing and no NPF was observed (off the
475 map in Figure 9b, see Figure 10). Nocturnal north-easterly breezes are often observed over the
476 Three Venetian Plain as a result of a low-level jet (Camuffo et al., 1979). The variability in local
477 wind fields may generate chemical gradients in the atmospheric surface layer within the Po Valley,
478 hence segregating air masses which can be active or inactive with respect to NPF, in complete
479 absence of orographic forcings (i.e. over a completely flat terrain). Probably the air masses with an
480 easterly component reaching the Zeppelin from the Venetian plain picked up pollution (e.g. CO,
481 NO_x) from urban sources, but we can also speculate that for example ammonia and amines were
482 much lower than in the westerly air masses flowing south of the Po river, which had crossed the
483 areas between Emilia and Lombardy where most agricultural activities take place (see Figure 10). A
484 chemical transport model run predicting NH₃ concentrations with adequate resolution, and using
485 them as a tracer for the actual precursors for NPF, might clarify this point. However modeling
486 atmospheric transport at this scale in an environment like Po Valley can have substantial
487 uncertainties (Vogel and Elbern, 2021).

488
489

490 **4 Conclusions**

491

492 Flight measurements are essential to evaluate the representativeness of the ground-based in-situ
493 measurements. In many cases it may be impossible to tell from only ground-based data what drives
494 the observed NPF, especially when the effect of BL dynamics is important. Atmospheric models
495 require field observations for validation and constraints. Airborne measurements such as the ones
496 reported here provide valuable data for this purpose.

497

498 We compared two different environments where NPF occurs frequently: a suburban area in Po
499 Valley, Italy, and a boreal forest in Hyytiälä, Finland. We aimed to answer in which part of the BL
500 the onset of NPF and the growth of the freshly formed particles takes place and studied the vertical
501 and horizontal extent of NPF.

502

503 To detect directly the very first steps of NPF in the BL, we used airborne Zeppelin and airplane
504 measurements, supported by ground-based in-situ measurements. The Zeppelin measurements



505 allowed us to study the vertical extent of NPF in the BL. The high time resolution and low cut-off
506 size of the instruments on board allowed us to observe the starting time, location and altitude of an
507 NPF event.

508

509 Within the limits of the Zeppelin's vertical profiling speed (~ 0.5 m/s ascend) and the time
510 resolution of the NAIS, we observed that the onset of NPF happened simultaneously inside the ML.
511 However particles formed close to the surface could probably still be mixed by strong updrafts fast
512 enough so that the number concentrations measured on board the Zeppelin appear homogeneous.
513 The newly formed particles were observed to grow to larger sizes at the same rate within the ML.
514 However, in HTL we observed local enhancements in NPF that were induced by roll vortices in the
515 BL.

516

517 In addition a separate layer of sub-10 nm particles was observed above the ML in HTL. Lampilahti
518 et al. (2020b) showed that such layers in HTL are likely the result of NPF in the topmost part of the
519 RL. Furthermore it was estimated that around 42% of the NPF events observed in HTL at the
520 surface are entrained from such elevated layers. In SPC we observed how NPF could be happening
521 in one air mass but be completely absent in an adjacent air mass with a different origin.

522

523 We presented three case studies (two from Italy and one from Finland). The conditions on our case
524 study days represent the typical conditions in these locations when NPF events usually occur. That
525 is to say, a sunny day with the air masses originating from a certain area during a period of the year
526 (May in HTL and June in SPC) when NPF is common. Nevertheless it is not certain that our case
527 studies represent all NPF event days. NPF events also occur under different kinds of conditions. The
528 growing nucleation mode particles originating from NPF do not always grow smoothly and
529 continuously in the measured size distribution like in our cases, but may have large variation and
530 discontinuities, which may reflect the vertical and horizontal variability in NPF.

531

532 **Acknowledgements**

533 This research was supported by the European Commission under the Framework Programme 7
534 (FP7-ENV-2010-265148). The support by the Academy of Finland Centre of Excellence program
535 (project no. 272041 and 1118615), the ERC-Advanced "ATMNUCLE" (grant no. 227463), the
536 Eurostars Programme (contract no. E!6911), and the Finnish Cultural Foundation is also gratefully
537 acknowledged. The Zeppelin is accompanied by an international team of scientists and technicians.
538 They are all warmly acknowledged.



539

540 **Data availability.** Ground-based meteorological data, radiation, gas and particle size distribution
541 data from HTL is available from <https://smear.avaa.csc.fi/> (last access: Apr 1, 2021). The Cessna
542 dataset is available from <https://doi.org/10.5281/zenodo.3688471> (last access: Oct 23, 2020). The
543 rest of the data used was gathered into another dataset: <https://doi.org/10.5281/zenodo.4660145>.

544

545 **Author contributions.** HM, TN, SM, ME, IP, SS, JKa, EJ, TYJ, RK, KLeh, SD, AM, RT, DW, FR,
546 TP, TM and MK coordinated the Zeppelin campaign. RV carried out the Cessna measurements. JLa,
547 TN, HM, JKo, KLei and VMK analyzed and interpreted the data. JL and HM prepared the
548 manuscript, with contributions from all coauthors.

549

550 **The authors declare that they have no conflict of interest.**

551



552

553 References

- Aalto, P., Hämeri, K., Becker, E., Weber, R., Salm, J., Mäkelä, J. M., Hoell, C., O'Dowd, C. D., Hansson, H.-C., Väkevä, M., Koponen, I. K., Buzorius, G. and Kulmala, M.: Physical characterization of aerosol particles during nucleation events, *Tellus B*, 53(4), 344–358, doi:10.3402/tellusb.v53i4.17127, 2001.
- Camuffo, D., Tampieri, F. and Zambon, G.: Local mesoscale circulation over Venice as a result of the mountain-sea interaction, *Bound.-Layer Meteorol.*, 16(1), 83–92, doi:10.1007/BF02220408, 1979.
- Chen, H., Hodshire, A. L., Ortega, J., Greenberg, J., McMurry, P. H., Carlton, A. G., Pierce, J. R., Hanson, D. R. and Smith, J. N.: Vertically resolved concentration and liquid water content of atmospheric nanoparticles at the US DOE Southern Great Plains site, *Atmospheric Chem. Phys.*, 18(1), 311–326, doi:https://doi.org/10.5194/acp-18-311-2018, 2018.
- Dal Maso, M., Kulmala, M., Riipinen, I., Wagner, R., Hussein, T., Aalto, P. P. and Lehtinen, K. E.: Formation and growth of fresh atmospheric aerosols: eight years of aerosol size distribution data from SMEAR II, Hyytiälä, Finland, *Boreal Environ. Res.*, 10(5), 323, 2005.
- Ehn, M., Junninen, H., Petäjä, T., Kurtén, T., Kerminen, V.-M., Schobesberger, S., Manninen, H. E., Ortega, I. K., Vehkamäki, H., Kulmala, M. and Worsnop, D. R.: Composition and temporal behavior of ambient ions in the boreal forest, *Atmospheric Chem. Phys.*, 10(17), 8513–8530, doi:https://doi.org/10.5194/acp-10-8513-2010, 2010.
- Ehn, M., Thornton, J. A., Kleist, E., Sipilä, M., Junninen, H., Pullinen, I., Springer, M., Rubach, F., Tillmann, R., Lee, B., Lopez-Hilfiker, F., Andres, S., Acir, I.-H., Rissanen, M., Jokinen, T., Schobesberger, S., Kangasluoma, J., Kontkanen, J., Nieminen, T., Kurtén, T., Nielsen, L. B., Jørgensen, S., Kjaergaard, H. G., Canagaratna, M., Maso, M. D., Berndt, T., Petäjä, T., Wahner, A., Kerminen, V.-M., Kulmala, M., Worsnop, D. R., Wildt, J. and Mentel, T. F.: A large source of low-volatility secondary organic aerosol, *Nature*, 506(7489), 476–479, doi:10.1038/nature13032, 2014.
- Eisele, F. L. and Tanner, D. J.: Ion-assisted tropospheric OH measurements, *J. Geophys. Res. Atmospheres*, 96(D5), 9295–9308, doi:10.1029/91JD00198, 1991.
- Hakola, H., Tarvainen, V., Laurila, T., Hiltunen, V., Hellén, H. and Keronen, P.: Seasonal variation of VOC concentrations above a boreal coniferous forest, *Atmos. Environ.*, 37(12), 1623–1634, doi:10.1016/S1352-2310(03)00014-1, 2003.
- Hamed, A., Joutsensaari, J., Mikkonen, S., Sogacheva, L., Maso, M. D., Kulmala, M., Cavalli, F., Fuzzi, S., Facchini, M. C., Decesari, S., Mircea, M., Lehtinen, K. E. J. and Laaksonen, A.: Nucleation and growth of new particles in Po Valley, Italy, *Atmospheric Chem. Phys.*, 7(2), 355–376, doi:https://doi.org/10.5194/acp-7-355-2007, 2007.
- Hari, P. and Kulmala, M.: Station for measuring ecosystem-atmosphere relations (SMEAR II), *Boreal Environ. Res.*, 10(5), 315–322, 2005.
- Junninen, H., Ehn, M., Petäjä, T., Luosujärvi, L., Kotiaho, T., Kostianen, R., Rohner, U., Gonin, M., Fuhrer, K., Kulmala, M. and Worsnop, D. R.: A high-resolution mass spectrometer to measure atmospheric ion composition, *Atmospheric Meas. Tech.*, 3(4), 1039–1053, doi:10.5194/amt-3-1039-2010, 2010.



Kerminen, V.-M., Chen, X., Vakkari, V., Petäjä, T., Kulmala, M. and Bianchi, F.: Atmospheric new particle formation and growth: review of field observations, *Environ. Res. Lett.*, 13(10), 103003, doi:10.1088/1748-9326/aadf3c, 2018.

Kontkanen, J., Järvinen, E., Manninen, H. E., Lehtipalo, K., Kangasluoma, J., Decesari, S., Gobbi, G. P., Laaksonen, A., Petäjä, T. and Kulmala, M.: High concentrations of sub-3nm clusters and frequent new particle formation observed in the Po Valley, Italy, during the PEGASOS 2012 campaign, , doi:http://dx.doi.org/10.5194/acp-16-1919-2016, 2016.

Kulmala, M., Petäjä, T., Nieminen, T., Sipilä, M., Manninen, H. E., Lehtipalo, K., Dal Maso, M., Aalto, P. P., Junninen, H., Paasonen, P., Riipinen, I., Lehtinen, K. E. J., Laaksonen, A. and Kerminen, V.-M.: Measurement of the nucleation of atmospheric aerosol particles, *Nat. Protoc.*, 7(9), 1651–1667, doi:10.1038/nprot.2012.091, 2012.

Kulmala, M., Kontkanen, J., Junninen, H., Lehtipalo, K., Manninen, H. E., Nieminen, T., Petäjä, T., Sipilä, M., Schobesberger, S., Rantala, P., Franchin, A., Jokinen, T., Järvinen, E., Äijälä, M., Kangasluoma, J., Hakala, J., Aalto, P. P., Paasonen, P., Mikkilä, J., Vanhanen, J., Aalto, J., Hakola, H., Makkonen, U., Ruuskanen, T., Mauldin, R. L., Duplissy, J., Vehkamäki, H., Back, J., Kortelainen, A., Riipinen, I., Kurten, T., Johnston, M. V., Smith, J. N., Ehn, M., Mentel, T. F., Lehtinen, K. E. J., Laaksonen, A., Kerminen, V.-M. and Worsnop, D. R.: Direct observations of atmospheric aerosol nucleation, *Science*, 339(6122), 943–946, doi:10.1126/science.1227385, 2013.

Laakso, L., Grönholm, T., Kulmala, L., Haapanala, S., Hirsikko, A., Lovejoy, E. R., Kazil, J., Kurten, T., Boy, M., Nilsson, E. D., Sogachev, A., Riipinen, I., Stratmann, F. and Kulmala, M.: Hot-air balloon as a platform for boundary layer profile measurements during particle formation, *Boreal Environ. Res.*, 12(3), 279–294, 2007.

Laaksonen, A., Hamed, A., Joutsensaari, J., Hiltunen, L., Cavalli, F., Junkermann, W., Asmi, A., Fuzzi, S. and Facchini, M. C.: Cloud condensation nucleus production from nucleation events at a highly polluted region, *Geophys. Res. Lett.*, 32(6), doi:10.1029/2004GL022092, 2005.

Lampilahti, J., Leino, K., Manninen, A., Poutanen, P., Franck, A., Peltola, M., Hietala, P., Beck, L., Dada, L., Quéléver, L., Öhrnberg, R., Zhou, Y., Ekblom, M., Vakkari, V., Zilitinkevich, S., Kerminen, V.-M., Petäjä, T. and Kulmala, M.: Aerosol particle formation in the upper residual layer, *Atmospheric Chem. Phys. Discuss.*, 1–24, doi:https://doi.org/10.5194/acp-2020-923, 2020a.

Lampilahti, J., Manninen, H. E., Leino, K., Väänänen, R., Manninen, A., Buenrostro Mazon, S., Nieminen, T., Leskinen, M., Enroth, J., Bister, M., Zilitinkevich, S., Kangasluoma, J., Järvinen, H., Kerminen, V.-M., Petäjä, T. and Kulmala, M.: Roll vortices induce new particle formation bursts in the planetary boundary layer, *Atmospheric Chem. Phys.*, 20(20), 11841–11854, doi:https://doi.org/10.5194/acp-20-11841-2020, 2020b.

Lehtipalo, K., Leppä, J., Kontkanen, J., Kangasluoma, J., Franchin, A., Wimmer, D., Schobesberger, S., Junninen, H., Petäjä, T., Sipilä, M., Mikkilä, J., Vanhanen, J., Worsnop, D. R. and Kulmala, M.: Methods for determining particle size distribution and growth rates between 1 and 3 nm using the Particle Size Magnifier, *Boreal Environ. Res.*, 19, 22, 2014.

Leino, K., Nieminen, T., Manninen, H. E., Petäjä, T., Kerminen, V.-M. and Kulmala, M.: Intermediate ions as a strong indicator for new particle formation bursts in boreal forest, *Boreal Environ. Res.*, 21, 274–286, 2016.



Leino, K., Lampilahti, J., Poutanen, P., Väänänen, R., Manninen, A., Buenrostro Mazon, S., Dada, L., Franck, A., Wimmer, D., Aalto, P. P., Ahonen, L. R., Enroth, J., Kangasluoma, J., Keronen, P., Korhonen, F., Laakso, H., Matilainen, T., Siivola, E., Manninen, H. E., Lehtipalo, K., Kerminen, V.-M., Petäjä, T. and Kulmala, M.: Vertical profiles of sub-3 nm particles over the boreal forest, *Atmospheric Chem. Phys.*, 19(6), 4127–4138, doi:10.5194/acp-19-4127-2019, 2019.

Manninen, H. E., Petäjä, T., Asmi, E., Riipinen, N., Nieminen, T., Mikkilä, J., Horrak, U., Mirme, A., Mirme, S., Laakso, L., Kerminen, V.-M. and Kulmala, M.: Long-term field measurements of charged and neutral clusters using Neutral cluster and Air Ion Spectrometer (NAIS), *Boreal Environ. Res.*, 14(4), 591–605, 2009.

Mirme, S. and Mirme, A.: The mathematical principles and design of the NAIS – a spectrometer for the measurement of cluster ion and nanometer aerosol size distributions, *Atmospheric Meas. Tech.*, 6(4), 1061–1071, doi:10.5194/amt-6-1061-2013, 2013.

Nieminen, T., Asmi, A., Dal Maso, M., Aalto, P. P., Keronen, P., Petäjä, T., Kulmala, M. and Kerminen, V.-M.: Trends in atmospheric new-particle formation: 16 years of observations in a boreal-forest environment, *Boreal Environ. Res.*, 19, 191–214, 2014.

Nieminen, T., Yli-Juuti, T., Manninen, H. E., Petäjä, T., Kerminen, V.-M. and Kulmala, M.: Technical note: New particle formation event forecasts during PEGASOS–Zeppelin Northern mission 2013 in Hyytiälä, Finland, *Atmospheric Chem. Phys.*, 15(21), 12385–12396, doi:10.5194/acp-15-12385-2015, 2015.

Nilsson, E. D., Paatero, J. and Boy, M.: Effects of air masses and synoptic weather on aerosol formation in the continental boundary layer, *Tellus B*, 53(4), 462–478, doi:10.1034/j.1600-0889.2001.530410.x, 2001a.

Nilsson, E. D., Rannik, Ü., Kulmala, M., Buzorius, G. and O’ Dowd, C. D.: Effects of continental boundary layer evolution, convection, turbulence and entrainment, on aerosol formation, *Tellus B*, 53(4), 441–461, doi:10.1034/j.1600-0889.2001.530409.x, 2001b.

O’Dowd, C. D., Yoon, Y. J., Junkermann, W., Aalto, P., Kulmala, M., Lihavainen, H. and Viisanen, Y.: Airborne measurements of nucleation mode particles II: boreal forest nucleation events, *Atmospheric Chem. Phys.*, 9(3), 937–944, doi:10.5194/acp-9-937-2009, 2009.

Platis, A., Altstädter, B., Wehner, B., Wildmann, N., Lampert, A., Hermann, M., Birmili, W. and Bange, J.: An Observational Case Study on the Influence of Atmospheric Boundary-Layer Dynamics on New Particle Formation, *Bound.-Layer Meteorol.*, 158(1), 67–92, doi:10.1007/s10546-015-0084-y, 2015.

Schobesberger, S., Väänänen, R., Leino, K., Virkkula, A., Backman, J., Pohja, T., Siivola, E., Franchin, A., Mikkilä, J., Paramonov, M., Aalto, P. P., Krejci, R., Petäjä, T. and Kulmala, M.: Airborne measurements over the boreal forest of southern Finland during new particle formation events in 2009 and 2010, *Boreal Environ. Res.*, 18(2), 145–164, 2013.

Siebert, H., Stratmann, F. and Wehner, B.: First observations of increased ultrafine particle number concentrations near the inversion of a continental planetary boundary layer and its relation to ground-based measurements, *Geophys. Res. Lett.*, 31(9), doi:10.1029/2003GL019086, 2004.



Sipilä, M., Berndt, T., Petäjä, T., Brus, D., Vanhanen, J., Stratmann, F., Patokoski, J., Mauldin, R. L., Hyvärinen, A.-P., Lihavainen, H. and Kulmala, M.: The Role of Sulfuric Acid in Atmospheric Nucleation, *Science*, 327(5970), 1243–1246, doi:10.1126/science.1180315, 2010.

Sogacheva, L., Hamed, A., Facchini, M. C., Kulmala, M. and Laaksonen, A.: Relation of air mass history to nucleation events in Po Valley, Italy, using back trajectories analysis, *Atmos Chem Phys*, 7(3), 839–853, doi:10.5194/acp-7-839-2007, 2007.

Sogacheva, L., Saukkonen, L., Nilsson, E. D., Dal Maso, M., Schultz, D. M., De Leeuw, G. and Kulmala, M.: New aerosol particle formation in different synoptic situations at Hyytiälä, Southern Finland, *Tellus B*, 60(4), 485–494, doi:10.1111/j.1600-0889.2008.00364.x, 2008.

Stein, A. F., Draxler, R. R., Rolph, G. D., Stunder, B. J. B., Cohen, M. D. and Ngan, F.: NOAA's HYSPLIT Atmospheric Transport and Dispersion Modeling System, *Bull. Am. Meteorol. Soc.*, 96(12), 2059–2077, doi:10.1175/BAMS-D-14-00110.1, 2015.

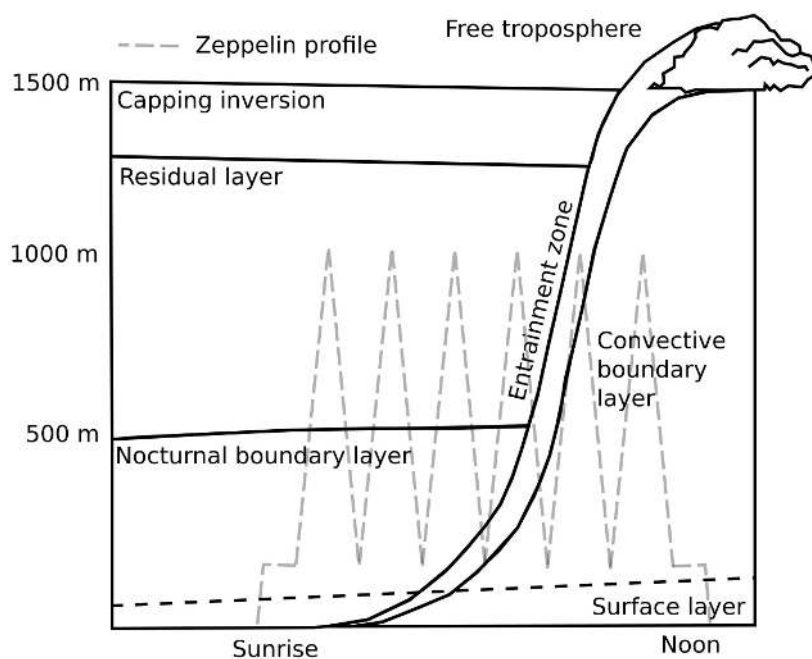
Stull, R. B.: *An Introduction to Boundary Layer Meteorology*, Softcover reprint of the original 1st ed. 1988 edition., Springer, Dordrecht., 1988.

Väänänen, R., Krejci, R., Manninen, H. E., Manninen, A., Lampilahti, J., Buenrostro Mazon, S., Nieminen, T., Yli-Juuti, T., Kontkanen, J., Asmi, A., Aalto, P. P., Keronen, P., Pohja, T., O'Connor, E., Kerminen, V.-M., Petäjä, T. and Kulmala, M.: Vertical and horizontal variation of aerosol number size distribution in the boreal environment, *Atmospheric Chem. Phys. Discuss.*, Manuscript in review, doi:10.5194/acp-2016-556, 2016.

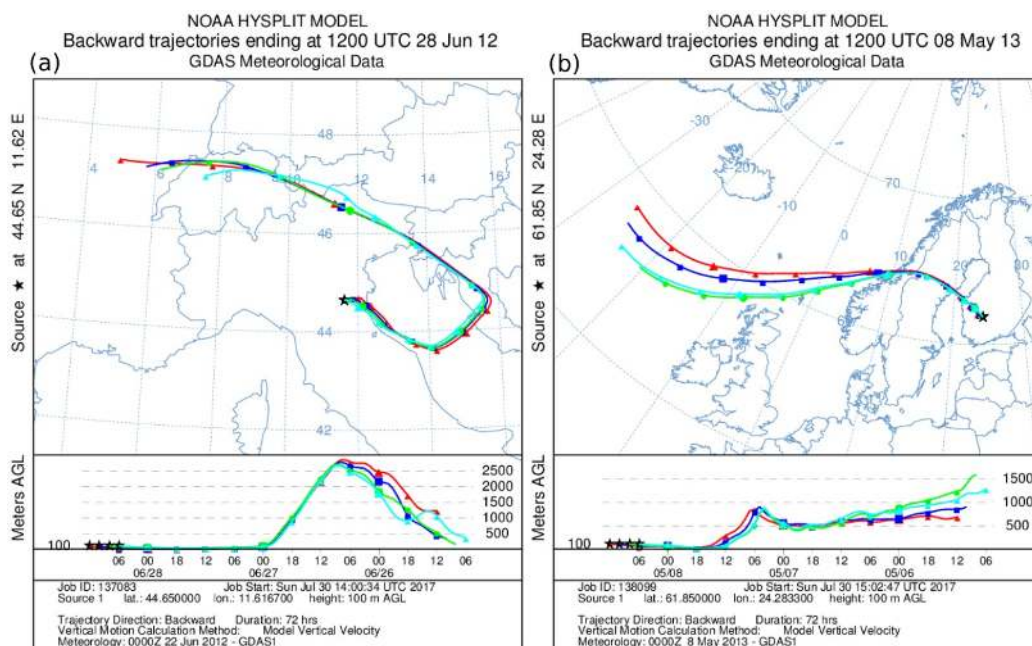
Vanhanen, J., Mikkilä, J., Lehtipalo, K., Sipilä, M., Manninen, H. E., Siivola, E., Petäjä, T. and Kulmala, M.: Particle size magnifier for nano-CN detection, *Aerosol Sci. Technol.*, 45(4), 533–542, doi:10.1080/02786826.2010.547889, 2011.

Wehner, B., Siebert, H., Ansmann, A., Ditas, F., Seifert, P., Stratmann, F., Wiedensohler, A., Apituley, A., Shaw, R. A., Manninen, H. E. and Kulmala, M.: Observations of turbulence-induced new particle formation in the residual layer, *Atmospheric Chem. Phys.*, 10(9), 4319–4330, doi:10.5194/acp-10-4319-2010, 2010.

Wiedensohler, A., Birmili, W., Nowak, A., Sonntag, A., Weinhold, K., Merkel, M., Wehner, B., Tuch, T., Pfeifer, S., Fiebig, M., Fjåraa, A. M., Asmi, E., Sellegri, K., Depuy, R., Venzac, H., Villani, P., Laj, P., Aalto, P., Ogren, J. A., Swietlicki, E., Williams, P., Roldin, P., Quincey, P., Hüglin, C., Fierz-Schmidhauser, R., Gysel, M., Weingartner, E., Riccobono, F., Santos, S., Gröning, C., Faloon, K., Beddows, D., Harrison, R., Monahan, C., Jennings, S. G., O'Dowd, C. D., Marinoni, A., Horn, H.-G., Keck, L., Jiang, J., Scheckman, J., McMurry, P. H., Deng, Z., Zhao, C. S., Moerman, M., Henzing, B., de Leeuw, G., Löschau, G. and Bastian, S.: Mobility particle size spectrometers: harmonization of technical standards and data structure to facilitate high quality long-term observations of atmospheric particle number size distributions, *Atmospheric Meas. Tech.*, 5(3), 657–685, doi:10.5194/amt-5-657-2012, 2012.

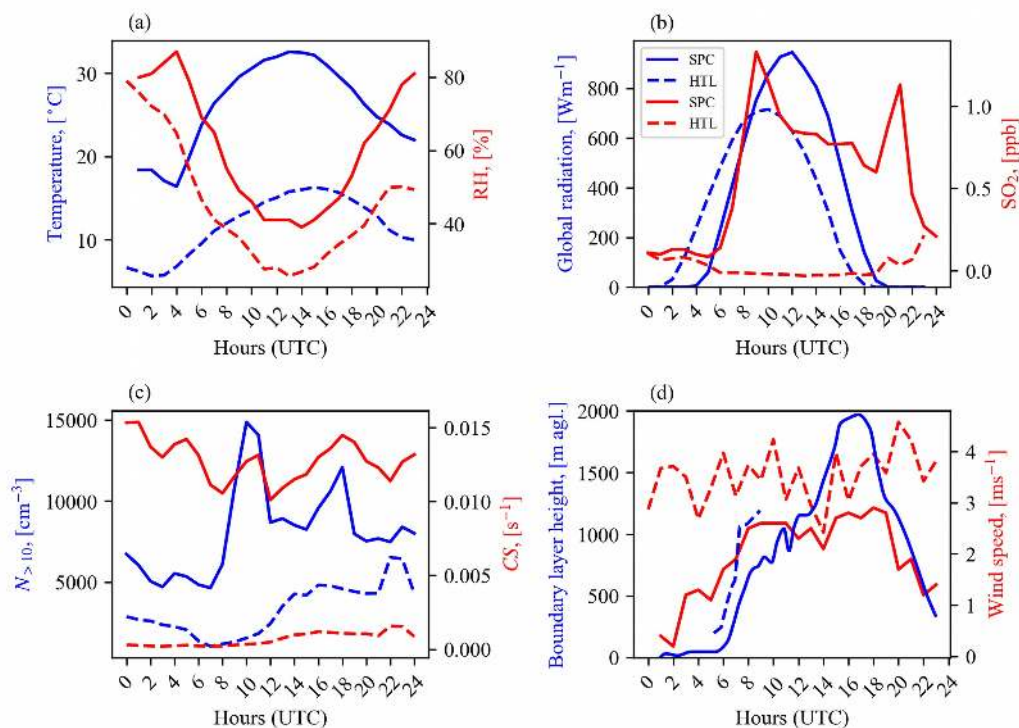


555 Figure 1: A schematic diagram of different atmospheric layers in the lower troposphere and their
556 development during the morning hours. A generic Zeppelin measurement profile (dashed gray line)
557 is displayed on top. The figure is adapted from Stull (1988).
558

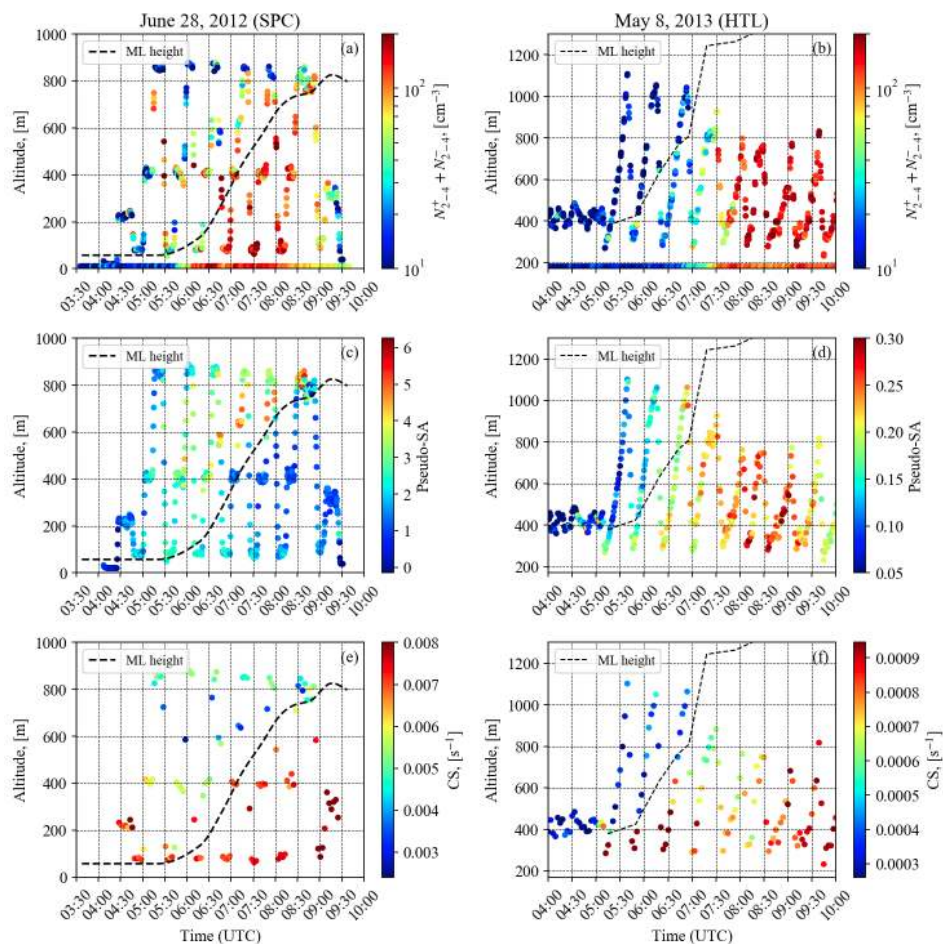


559 Figure 2: Air mass backward trajectories to (a) SPC during the morning of June 28, 2012 and (b)

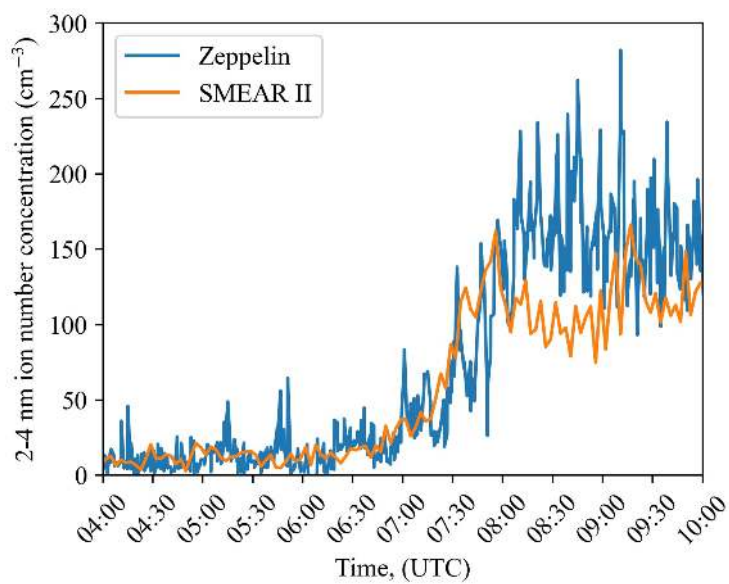
560 HTL during the morning of May 8, 2013.



561 Figure 3: Diurnal variation in (a) temperature, relative humidity, (b) global radiation, SO_2
562 concentration, (c) >10 nm particle number concentration, condensation sink (CS) and (d) mixed
563 layer height in SPC on June 28, 2012 and in HTL on May 8, 2013.
564



565 Figure 4: Time-evolution of selected variables as a function of height in SPC and HTL. Panels (a)
 566 and (b) show the intermediate ion number concentration from SPC and HTL. Ground-based
 567 measurements as well as measurements from the Zeppelin are shown. Panels (c) and (d) show the
 568 pseudo-SA from SPC and HTL. Panels (e) and (f) show the CS. Height of the mixed layer is shown
 569 in all panels.

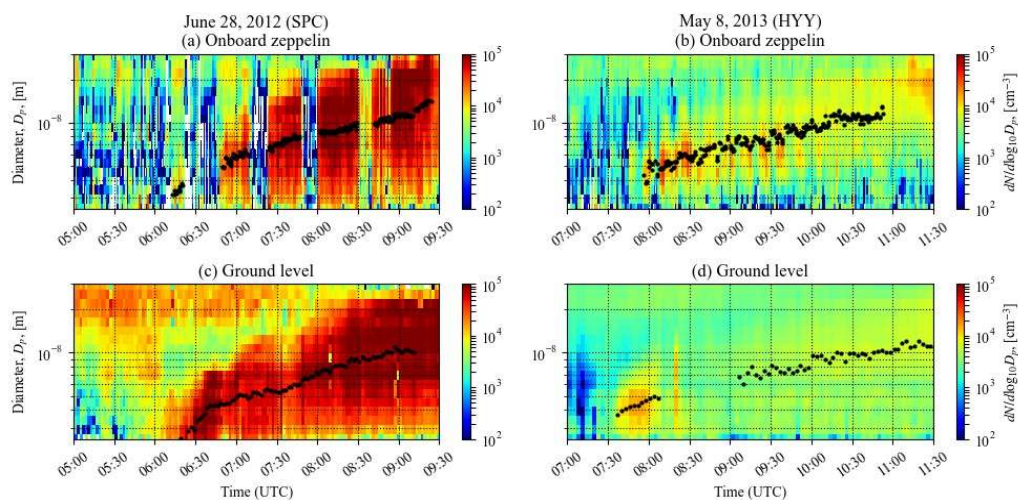


570 Figure 5: Time series of intermediate (2-4 nm) ion number concentration on board the Zeppelin and
571 the SMEAR II station in HTL on May 8, 2013.



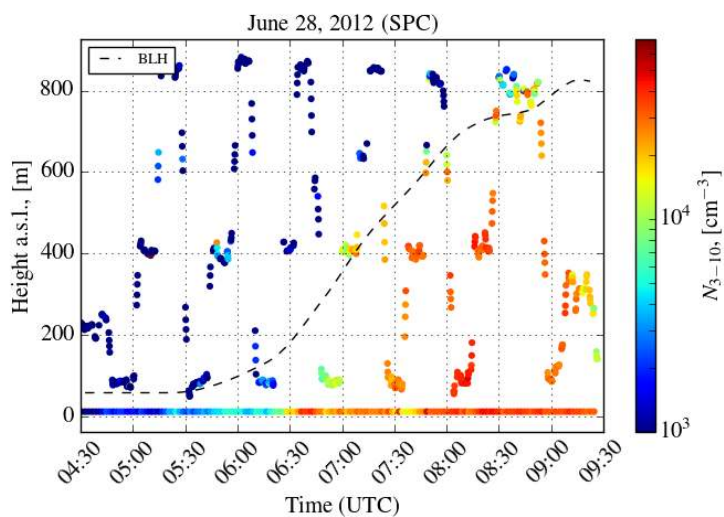
572

573

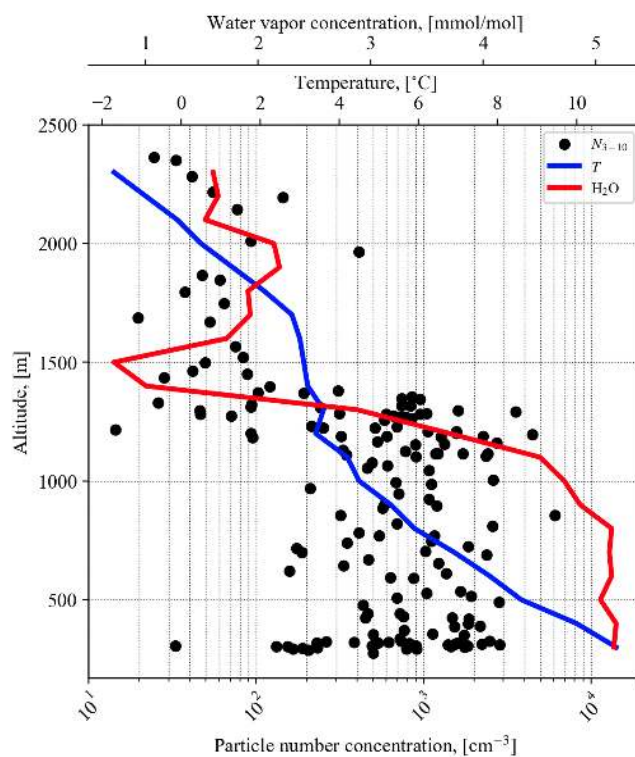


574 Figure 6. Time evolution of particle number size distributions measured by the NAIS (positive
575 polarity) on board the Zeppelin (a, b) and at the ground level (c, d) in HTL and in SPC on the two
576 case study days. The black dots are the mean mode diameters found by fitting a log-normal
577 distribution over the growing mode.

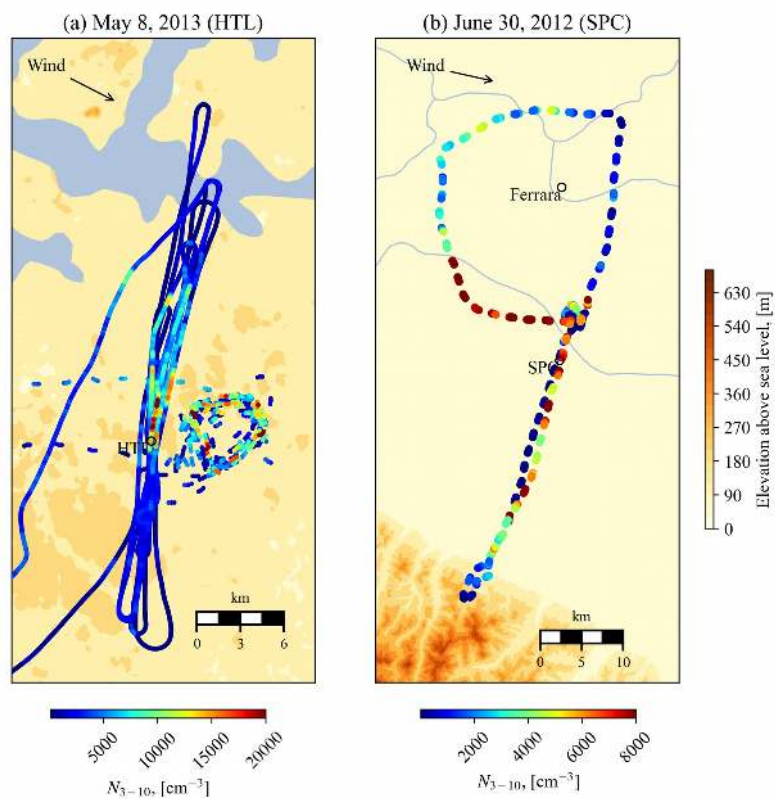
578



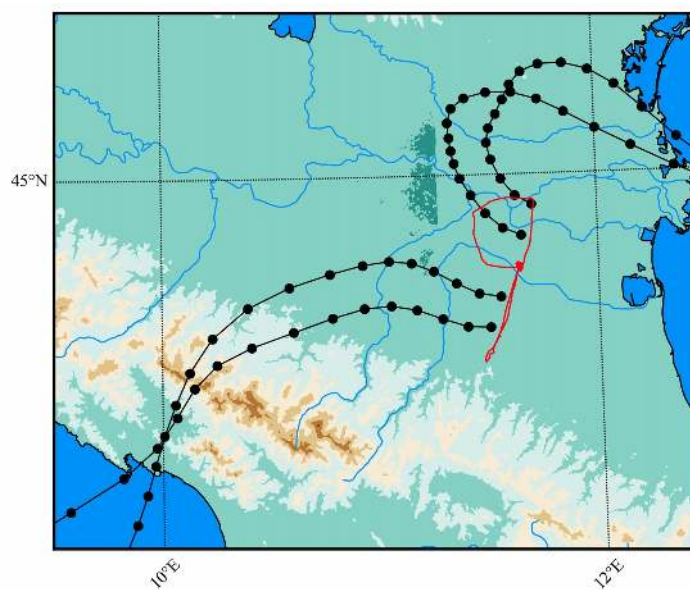
579 Figure 7. The particle number concentration in the 3-10 nm size range from SPC on board the
580 Zeppelin and on the ground level on June 28, 2012. BLH refers to the boundary layer height
581 determined from ceilometer.
582



583 Figure 8: Vertical profile of 3-10 nm particle number concentration (black dots), temperature (blue
584 line) and water vapor concentration (red line) measured on board the Cessna between 07:00-10:00
585 on May 8, 2013 in HTL.



586 Figure 9: (a) the flight tracks of the Zeppelin (circular track) and the airplane (track with back and
587 forth segments) colored by 3-10 nm particle number concentration from HTL on May 8, 2013. (b)
588 the flight track of the Zeppelin colored by 3-10 nm particle number concentration from SPC on June
589 30, 2012. The Zeppelin flight track has gaps because the NAIS was measuring in the ion mode
590 during that time.
591



592 Figure 10: Airmass back trajectories (black dotted lines) arriving to the Zeppelin's measurement
593 area over north Italy on June 30, 2012. The separation between the dots along the trajectories is one
594 hour. The red line is the Zeppelin's flight track.



595 Table 1. Calculated particle formation and growth rates. + and – superscripts refer to positive and
596 negative ions respectively. The Zeppelin missed the beginning of the NPF event in SPC and because
597 of that some values are missing.

598

	HTL (May 8, 2013)		SPC (June 28, 2012)	
	Zeppelin	Ground	Zeppelin	Ground
$J_{1.5}$, [$\text{cm}^{-3} \text{s}^{-1}$]	1.5	0.9	-	-
J_3 , [$\text{cm}^{-3} \text{s}^{-1}$]	0.2	0.3	-	6.8
J_3^- , [$\text{cm}^{-3} \text{s}^{-1}$]	0.04	0.04	-	0.04
J_3^+ , [$\text{cm}^{-3} \text{s}^{-1}$]	0.04	0.04	-	0.03
GR_{1-2} , [nm h^{-1}]	0.8	0.7	-	0.5
GR_{2-3} , [nm h^{-1}]	1.4	1.5	1.8	1.5
GR_{3-7} , [nm h^{-1}]	1.7	1.6	2.9	2.0
GR_{7-20} , [nm h^{-1}]	2.4	2.1	3.0	2.8

599